Automatica, Volume 141, July 2022, Article number 110294
DOI:10.1016/j.automatica.2022.110294

Stable Robot Manipulator Parameter Identification: A Closed-Loop Input Error Approach

Adolfo Perrusquía [a,⋆], Ruben Garrido [b], Wen Yu [b]

[a] *School of Aerospace, Transport and Manufacturing, Cranfield University, Bedford MK43 0AL*

[b] *Departamento de Control Automático, CINVESTAV-IPN (National Polytechnic Institute), Av. IPN 2508, Mexico City, 07360, Mexico.*

Abstract

This paper presents an on-line parametric estimation method for robot manipulators. The identification algorithm estimates the parameters by using the input error between the robot and a parallel estimated model. Both, the robot and the estimated model are controlled by two Proportional-Derivative (PD) controller tuned with the same gain values, and a persistent excitation (PE) signal for ensuring parameters convergence is included. The exact model matching and the estimation error cases are analysed. Noisy state measurements and filters are avoided in the model parameterization by using only the states of the estimated model. A second parameter identification algorithm, which is based on a composite update law, is also proposed. It improves parameters convergence and robustness of the update rule in presence of estimation errors. The stability of the closed-loop dynamics related to the estimated model is assessed via Lyapunov stability theory. Simulations are carried out to validate the proposed approaches.

Key words: System identification, CLIE, persistent exciting signal, composite update rule, estimation error, parameter convergence, gradient method.

1 Introduction

Parameter identification of robot manipulators is a well-known problem and it is a key component in the design of model-based controllers for these systems [13,37,27]. Its aim is to estimate a set of parameters depending on the robot physical parameters including link lengths, masses and moments of inertia, joint friction coefficients and gravitational terms.

There exist several motivations for developing parameter identification methods tailored to robot manipulators. Their dynamics are usually described by a set of coupled nonlinear differential equations. Moreover, in many cases only joint position and velocity measurements are available and acceleration measurements, which are required in some approaches, are absent in commercial available robots. Regarding the first issue, many of the classic parameter identification methods have been developed for discrete-time Linear Time Invariant (LTI) systems [17,8,20], and applying them to robot manipulators would require a discrete-time model of their dynamics. In this regard, there are very few works on discrete-time models for robot manipulators and its use for parameter identification has not yet been explored. Early work [21] shows a discrete-time nonlinear robot model obtained considering a constant inertia matrix, an assumption which may be unrealistic in practice, in particular for robots having only rotational joints. On the other hand, acceleration measurements are not available in industrial robots. A way to circumvent this problem is to add external accelerometers. However, these devices measure linear acceleration and in most cases the robot joints are rotational and thus angular acceleration measurements are needed. Moreover, data fusion from position encoders, gyroscopes and linear accelerometers together with Kalman filtering are needed to obtain joint angular velocity and acceleration estimates [19]. Besides, acceleration measurements are biased and possess large levels of measurement noise thus making filtering and signal processing necessary. To avoid angular acceleration measurements, one could resort to techniques applied to continuous-time LTI systems to obtain linear parametrizations of the robot model [5]. In this case, a filtering procedure avoids the measurement of the time

⋆ Corresponding author Adolfo Perrusquía.
Email address:
Adolfo.Perrusquia-Guzman@cranfield.ac.uk (Adolfo Perrusquía).

derivatives of the system input and output. However, their usefulness in parameter identification of robot manipulators is limited by the nonlinearities appearing in their models.

An account of the identification methods developed for robot manipulators and proposed in the literature is described next. One of the most widely studied approaches is the IDIM-LS method, which is based on the Inverse Dynamic model (IDIM) of a robot manipulator coupled with the Least Squares (LS) or some of its variants [38,39,11,41,10,12]. A feature of this method is the fact that each robot joint is first stabilized through a Proportional Derivative (PD) or a Proportional Integral Derivative (PID) controller. Then, the robot measured input torques, the joint positions and in some cases the joint velocities feed a Least Squares algorithm. A filtered IDIM and the LS algorithm has been proposed in [31] where the robot Supplied Energy Model (SEM), identified using the LS algorithm, is also studied. Flexible joint robot manipulators have been identified using an IDIM filtered model coupled with an LS algorithm [18]. In the IDIM-IV method an Instrumental Variable (IV) algorithm replaces the standard LS algorithm, and the identified model corresponds to the IDIM [9].

An alternative approach to the above methods is the use of Closed-Loop Output Error (CLOE) algorithms. The idea dates back to the parameter identification of discrete-time linear systems [15]. The CLOE methods are based on a parallel model structure in which the robot and its model are simultaneously controlled by PD controllers tuned with the same gains and fed by the same excitation signal. The parameters of the model are tuned through a parameter estimation algorithm like the LS method, which is driven by the error between the position of the robot and the simulated position generated by the robot model. Unlike the IDIM-based methods, the signals generated by the model feed the identification algorithm thus avoiding measurement noise problems. The above configuration produces a nonlinear closed-loop system composed by the robot model, the PD controller and the parameter identification algorithm. Examples of approaches exploiting this idea are found in [2,7].

The Closed-Loop Input Error (CLIE) method [2], is the counterpart of the CLOE method and retains the same parallel topology. However, in this case the robot position error is replaced by the error between the real robot torque and the torque generated by the model. It is particularly interesting reference [7], which describes most of the approaches used for parameter identification of robot manipulators. That work also reports the Direct and Inverse Dynamic Identification Model (DIDIM) method which shares some of the features of the CLIE method and uses a nonlinear LS algorithm for parameter identification. A problem faced by this approach is the choice of the initial parameter estimates, which may require prior knowledge on the robot parameters.

It is also worth to note that parameter identification of robot manipulators may be performed as a part of an adaptive controller [29] as in the case of the classic and widely known Slotine-Li algorithm [34,40,42,24].

In spite of the successful implementation of the CLOE and CLIE methods for the parameter identification of robot manipulators, the theoretical question about the stability of the nonlinear closed-loop system resulting from the robot model, the PD controller and the parameter identification algorithm remains open. In other words, the boundedness of the trajectories of the simulated model whose parameters are updated through an LS or a VI method has not been theoretically proved even if the experimental results produce good parameter estimates. Moreover, there are no studies showing how the previous CLIE and CLOE algorithms are affected by bounded estimation errors.

Motivated by the above comments, this work reports a CLIE algorithm in which the stability problem previously mentioned is solved. The approach is related to previous work on parameter identification of servo systems [6].

The main features of the proposed CLIE algorithm are the following

(1) Rigorous stability and parameter convergence results related to the estimated model using Lyapunov stability theory and results on based on Persistency of Excitation conditions are given to support the proposed approach.
(2) The regressor matrix used in the proposed update law depends only on the signals produced by a model, which are noise-free and consequently avoids the use of measurements of joint positions and velocities that may be contaminated by noise.
(3) A robustness analysis of the CLIE algorithm is presented by considering bounded estimation errors and Persistency of Excitation conditions.
(4) A modification of the update law of the CLIE algorithm called the composite update law, and aimed to improve parameter convergence, adds a term depending on an identification error.

The contributions of this work with respect to previous developments for parameter identification of robot manipulators based on CLIE and CLOE algorithms are the following:

- The proposed CLIE algorithm is supported by a rigorous stability proof, which proves that all the signals in the nonlinear closed-loop system resulting from the robot model, the PD controller and the update law are bounded under zero and non-zero bounded estimation error conditions.

- Parameter convergence is also rigorously demonstrated by considering Persistency of Excitation conditions also under zero and non-zero bounded estimation error conditions.
- The algorithm is simple to put to work since only a gain in the update law for each robot joint needs tuning while in the case of the composite update law two gains need tuning, and unlike some previous methods the parameter estimates initial conditions may be freely set.

The paper outline is as follows: Section II presents the robot dynamics including the actuators gear trains. Section III defines the CLIE algorithm for robot manipulator identification where the update rule and exponential convergence is proved via Lyapunov theory. Section IV introduces the CLIE algorithm based on a composite update law using a gradient algorithm. Section V reports simulations studies using a 2-DOF robot. The conclusions are presented in Section VI.

Throughout this paper, $\mathbb{N}$, $\mathbb{R}$, $\mathbb{C}$, $\mathbb{R}^+$, $\mathbb{R}^n$, $\mathbb{R}^{n\times m}$ denote the spaces of natural numbers, real numbers, complex numbers, positive real numbers, real n-vectors, and real $n \times m$-matrices, respectively; $I \in \mathbb{R}^{n\times n}$ denotes an identity matrix; $\mathcal{L}_\infty$ denotes the space of bounded signals, $\mathcal{L}_2$ denotes the space of square integrable functions, $\lambda_{\min}(A)$ and $\lambda_{\max}(A)$ denotes the minimum and maximum eigenvalues of matrix A, respectively; $\text{diag}\,(\cdot)$ denotes a diagonal matrix, the norms $\|A\| = \sqrt{\lambda_{\max}(A^\top A)}$ and $\|x\|$ stand for the induced matrix and vector Euclidean norms, respectively; $\max(\cdot)$ denote the maximum operator, $A > 0$ denotes a positive definite matrix, and $A > B$ means that $A - B$ is positive definite; where $x \in \mathbb{R}^n$, $A, B \in \mathbb{R}^{n\times n}$ and $n, m \in \mathbb{N}$.

2 Robot dynamics of n-DOF with actuator/gear train

The robot dynamics of a n-DOF robot is obtained by the Euler-Lagrange formulation and is given by [37]

$$M(q)\ddot{q} + C(q,\dot{q})\dot{q} + H\dot{q} + G(q) = \tau + \delta_r, \qquad (1)$$

where $M(q) \in \mathbb{R}^{n\times n}$ is a symmetric and positive definite inertia matrix, $C(q,\dot{q}) \in \mathbb{R}^{n\times n}$ stands for the Coriolis and centrifugal forces/torques matrix, $H \in \mathbb{R}^{n\times n}$ is a diagonal viscous friction matrix, $G(q) \in \mathbb{R}^n$ is the gravitational torques vector, δ_r is a vector of bounded disturbances, $\tau \in \mathbb{R}^n$ is the input torques vector, and $q, \dot{q}, \ddot{q} \in \mathbb{R}^n$ are the position, velocity and acceleration vectors, respectively. The robot dynamics (1) may also be written as

$$\sum_{j=1}^{n} m_{jk}(q)\ddot{q}_j + \sum_{i,j=1}^{n} c_{ijk}\dot{q}_i\dot{q}_j + h_{kk}\dot{q}_k + g_k(q) = \tau_k + \delta_{kr},$$

or equivalently as

$$m_{kk}(q)\ddot{q}_k + h_{kk}\dot{q}_k + \eta_k = \tau_k + \delta_{kr}, k = 1, \ldots, n \qquad (2)$$

where

$$\eta_k = \sum_{j\neq k}^{n} m_{jk}(q)\ddot{q}_j + \sum_{i,j=1}^{n} c_{ijk}\dot{q}_i\dot{q}_j + g_k(q) \qquad (3)$$

Then, η_k lumps the off-the-diagonal nonlinear coupling terms of the robot model (1) and is assumed as a time-varying bounded disturbance.

The mechanical model of each DC motor k driving the robot joints through a gearbox is given by

$$J_k\ddot{\theta}_k + R_k\dot{\theta}_k = u_k - \frac{\tau_k}{r_k} + \delta_{km} \qquad (4)$$

where J_k is the motor inertia, R_k is the motor viscous friction coefficient, u_k is the control input, δ_{km} accounts for bounded disturbances, r_k is the k-th gear ratio and θ_k, $\dot{\theta}_k$ $\ddot{\theta}_k \in \mathbb{R}$ are the motor angular position, velocity and acceleration. A high gear ratio r_k decouples the robot dynamics by reducing the effect of the off-the-diagonal terms in the robot model on the DC motors. Typical values of r_k are 200-500. On the other hand, the joint and motor angular positions are related by

$$q_k = \frac{\theta_k}{r_k}. \qquad (5)$$

Using the above formula and (4) allow obtaining the next set of decoupled linear models for each robot joint

$$\mathcal{J}_k\ddot{q}_k + \mathcal{R}_k\dot{q}_k + d_k = u_k \qquad (6)$$

where $\mathcal{J}_k = J_k r_k + \frac{1}{r_k} m_{kk}(q)$, $\mathcal{R}_k = R_k r_k + \frac{h_{kk}}{r_k}$ and

$$d_k = \frac{\eta_k - \delta_{kr}}{r_k} - \delta_{km}. \qquad (7)$$

Notice that the term $\mathcal{J}_k$ is composed of the inertia of the k-th DC motor and the kk-th diagonal term of the robot matrix inertia divided by the gear ratio r_k. Hence, for large values of r_k the term $\frac{1}{r_k} m_{kk}(q)$ is small and $\mathcal{J}_k$ is approximately constant. On the other hand, a large gear ratio r_k also renders the quotient h_{kk}/r_k small and therefore the term $\mathcal{R}_k$ is dominated by the DC motor viscous friction coefficient R_k. Moreover, note in (6) that whilst the effect of the DC motor dynamics increases proportionally with r_k, the terms associated to the robot dynamics including η_k and δ_{kr} are proportionally attenuated by the inverse of r_k. The diagram of each joint k is given in Fig. 1 in closed-loop with a PD controller.

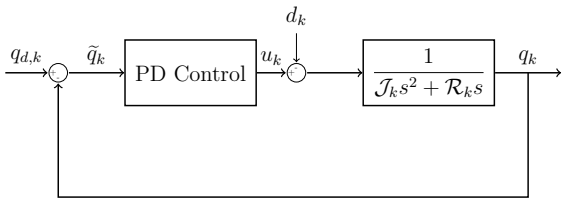

Fig. 1. Diagram of each robot joint in closed-loop with a PD controller.

Therefore, the corresponding matrix-vector model of the perturbed robot dynamics is

$$\mathcal{J}\ddot{q} + \mathcal{R}\dot{q} + d = u \tag{8}$$

where $\mathcal{J} \in \mathbb{R}^{n\times n}$ is a constant diagonal inertia matrix, $\mathcal{R} \in \mathbb{R}^{n\times n}$ is a diagonal viscous friction matrix, $d \in \mathbb{R}^n$ is a bounded disturbance vector and $u \in \mathbb{R}^n$ is the control input vector.

Now consider the following alternative form of the robot dynamics (8)

$$\ddot{q} = -A\dot{q} + Bu - D \tag{9}$$

where A and B are diagonal positive definite matrices defined as $A = \mathcal{J}^{-1}\mathcal{R}$, $B = \mathcal{J}^{-1}$, and $D = \mathcal{J}^{-1}d$.

Each component of the vector D is given by

$$D_k = \frac{1}{\mathcal{J}_k}\left[\frac{\eta_k - \delta_{kr}}{r_k} - \delta_{km}\right] \tag{10}$$

Assume that the disturbances δ_{km} are constant. Notice that a large gear ratio r_k attenuates the effect of the off-the-diagonal nonlinear coupling terms η_{kr} and the disturbance δ_{kr}. Consequently, the term D_k depends essentially on $\delta_{km}/\mathcal{J}_k$. These conditions permit assuming that the terms D_k and thus the vector D in (9) are constant.

3 Closed loop input error (CLIE) identification technique

A block diagram of the CLIE algorithm is depicted in Fig. 2. The robot and its model are controlled using the same PD controller and the error between their outputs feeds an identification algorithm that subsequently updates the estimated model.

Consider the next PD control law applied to the dynamics (9)

$$u = K_p\tilde{q} - K_d\dot{q} + PE, \tag{11}$$

where $K_p, K_d \in \mathbb{R}^{n\times n}$ are diagonal and positive definite matrices and correspond to the proportional and derivative gains, respectively, defined as $K_p = \text{diag}\,(k_{p_1}, \cdots, k_{p_n})$ and $K_d = \text{diag}\,(k_{d_1}, \cdots, k_{d_n})$, where $k_{p_i}, k_{d_i} > 0$, $i = 1, \cdots n$ are the diagonal elements

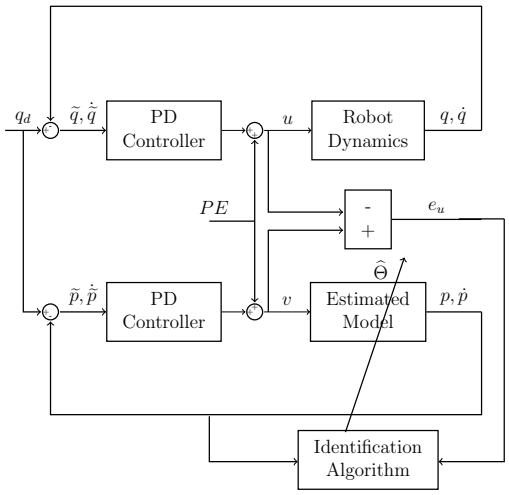

Fig. 2. Block diagram of the closed-loop input identification technique

of the proportional and derivative gain, respectively, $\tilde{q} = q_d - q$ is a position error, $q_d \in \mathbb{R}^n$ is a constant desired reference and PE is a bounded persistent excitation signal.

The dynamics (9) under the control law (11) yields the closed-loop dynamics

$$\ddot{q} = -(A + BK_d)\dot{q} + B(K_p\tilde{q} + PE) - D = -\Phi^\top\Theta \tag{12}$$

where $\Phi = \Phi(\tilde{q}, \dot{q}, PE) \in \mathbb{R}^{p\times n}$ is the regressor matrix and $\Theta \in \mathbb{R}^p$ is the unknown parameters vector which are defined as

$$\Phi = \begin{bmatrix} \text{diag}\,(\dot{q}_i)_{i=1}^n \\ -\text{diag}\,(K_{p_i}\tilde{q}_i - K_{d_i}\dot{q}_i + PE_i)_{i=1}^n \\ I \end{bmatrix},\ \Theta = \begin{bmatrix} A\cdot\vec{1} \\ B\cdot\vec{1} \\ D \end{bmatrix} \tag{13}$$

where $\vec{1} = \begin{bmatrix} 1 & \dots & 1 \end{bmatrix}^\top \in \mathbb{R}^n$.

The following Lyapunov function is used to verify the Uniform Ultimate Boundedness (UUB, also known as practical stability) [14] of the closed-loop trajectories of (12) under the effect of bounded disturbances [22,30,28].

$$V = \frac{1}{2}\dot{q}^\top\dot{q} + \frac{1}{2}\tilde{q}^\top\left(\frac{1}{2}W^2 + BK_p\right)\tilde{q} - \frac{1}{2}\tilde{q}^\top W\dot{q}, \tag{14}$$

where $W = A + BK_d$ and $BK_p > 0$. It is easy to check that (14) is positive definite by writing V as

$$\begin{aligned} V = \frac{1}{2}\Big[&\Big(\dot{q} - \frac{1}{2}W\tilde{q}\Big)^\top\Big(\dot{q} - \frac{1}{2}W\tilde{q}\Big) \\ &+\tilde{q}^\top\Big(\frac{1}{4}W^2 + BK_p\Big)\tilde{q}\Big] \end{aligned} \tag{15}$$

The time-derivative of (14) along the closed-loop trajectories of (12) is

$$\begin{aligned}\dot{V} =& -\frac{1}{2}\dot{q}^\top W\dot{q} - \frac{1}{2}\widetilde{q}^\top WBK_p\widetilde{q} + \dot{q}^\top\eta - \frac{1}{2}\widetilde{q}^\top W\eta \\ \dot{V} \leq& -\frac{1}{2}\lambda_{\min}(W)\|\dot{q}\|^2 - \frac{1}{2}\lambda_{\min}(WBK_p)\|\widetilde{q}\|^2 \\ &+ \|\dot{q}\|\|\eta\| + \frac{1}{2}\lambda_{\max}(W)\|\widetilde{q}\|\|\eta\| \end{aligned} \tag{16}$$

where $\eta = BPE - D$. The inequality (16) can be written as

$$\begin{aligned}\dot{V} \leq& -x^\top\mathcal{A}x + \|\eta\|\mathcal{B}^\top x \\ \leq& -\lambda_{\min}(\mathcal{A})\|x\|\left[\|x\| - \frac{\|\mathcal{B}\|\|\eta\|}{\lambda_{\min}(\mathcal{A})}\right]\end{aligned} \tag{17}$$

where $x = [\dot{q}^\top\ \widetilde{q}^\top]^\top$, $\mathcal{A} = \frac{1}{2}\text{diag}\{\lambda_{\min}(W), \lambda_{\min}(WBK_p)\}$, and $\mathcal{B} = [1\ \frac{1}{2}\lambda_{\max}(W)]^\top$. Therefore, $\dot{V} < 0$ as long as

$$\|x\| \geq \frac{\|\mathcal{B}\|\|\eta\|}{\lambda_{\min}(\mathcal{A})} \equiv \mu_0 \tag{18}$$

Selecting positive control gains K_p and K_d such that (18) is satisfied ensures that the trajectories of system (12) converge to a compact set S_x of radius μ_0, i.e., $\|x\| \leq \mu_0$ and hence, the trajectories of (12) are UUB.

Remark 1 *The above result shows that a simple PD controller stabilizes (in a practical stability sense) the robot manipulator without explicit knowledge on its parameters. An advantage of this controller is that it is easy to tune [4,22]. Note that there exists an steady state error due to the bounded disturbances. In this regard, a PID controller [43] could be used to reduce the steady state error by means of the integral term. However, the only restriction on the robot controller imposed by the parameter identification approach proposed here is to guarantee a stable closed-loop dynamics of the real robot without regard on the tracking quality of the closed-loop system. Thus, an integral action is not needed. Moreover, adding an integrator further complicates the stability analysis [26] and the controller tuning, and opens the possibility of windup phenomena.*

3.1 Exact Model Matching

Consider an estimated model whose structure matches the robot dynamics (9)

$$\ddot{p} = -\widehat{A}\dot{p} + \widehat{B}v - \widehat{D} \tag{19}$$

where $\widehat{A}, \widehat{B}, \widehat{D}$ are estimates of A, B and D, respectively, and $p \in \mathbb{R}^n$ is the model state. Let the following PD control law applied to (19) be

$$v = K_p\widetilde{p} - K_d\dot{p} + PE \tag{20}$$

with $\widetilde{p} = q_d - p$. Notice that (11) and (20) use the same values of the gain matrices and the persistent signal PE. The system dynamics (19) under the control law (20) yields the closed loop dynamics

$$\ddot{p} = -(\widehat{A} + \widehat{B}K_d)\dot{p} + \widehat{B}(K_p\widetilde{p} + PE) - \widehat{D} = -\Phi_p^\top\widehat{\Theta}. \tag{21}$$

The term $\Phi_p = \Phi_p(\widetilde{p}, \dot{p}, PE) \in \mathbb{R}^{p\times n}$ is a regressor matrix and $\widehat{\Theta} \in \mathbb{R}^p$ is an estimate of the parameter vector Θ which are defined as

$$\Phi_p = \begin{bmatrix} \text{diag}\,(\dot{p}_i)_{i=1}^n \\ -\text{diag}\,(K_{p_i}\widetilde{p}_i - K_{d_i}\dot{p}_i + PE_i)_{i=1}^n \\ I \end{bmatrix},\ \widehat{\Theta} = \begin{bmatrix} \widehat{A}\cdot\vec{1} \\ \widehat{B}\cdot\vec{1} \\ \widehat{D} \end{bmatrix}. \tag{22}$$

Note that the regressor Φ_p depends on the state of the estimated model instead of the state of the robot dynamics. Then, all the signals in the regressor are noise-free. Define the output error as

$$e = \widetilde{p} - \widetilde{q} = q - p \tag{23}$$

Under this new coordinates the closed-loop error dynamics between the dynamics (9) and the estimated model (19) are

$$\begin{aligned}\ddot{e} &= -\bar{A}\dot{e} - \bar{B}e + \widetilde{A}\dot{p} - \widetilde{B}v + \widetilde{D} \\ &= -\bar{A}\dot{e} - \bar{B}e + \Phi_p^\top\widetilde{\Theta}\end{aligned} \tag{24}$$

where $\bar{A} = A + BK_d$, $\bar{B} = BK_p$, $\widetilde{\Theta} = \widehat{\Theta} - \Theta \in \mathbb{R}^p$ is the parametric error vector. The parametric error is defined as

$$\widetilde{\Theta} = \widehat{\Theta} - \Theta = \begin{bmatrix} (\widehat{A} - A)\cdot\vec{1} \\ (\widehat{B} - B)\cdot\vec{1} \\ \widehat{D} - D \end{bmatrix}. \tag{25}$$

The input error e_u is defined by

$$\begin{aligned}e_u &= v - u \\ &= K_p e + K_d\dot{e}\end{aligned} \tag{26}$$

The following theorem establishes the stability and parameter convergence of the CLIE approach applied to parameter estimation of robot manipulators.

Theorem 1 *Consider the robot dynamics (9) in closed-loop with the PD control law (11), and the estimated*

model (19) in closed-loop with control law (20). If the parameter estimates $\widehat{\Theta}$ are updated as

$$\dot{\widehat{\Theta}} = -\Gamma \Phi_p K_d K_p^{-1} e_u, \tag{27}$$

where $\Gamma \in \mathbb{R}^{p\times p}$ is a positive definite matrix gain, and $K_p^{-1}K_d\bar{A} - I > 0$ then $\widetilde{\Theta}$, e, $\dot{e}$, p, $\dot{p}$ and Φ_p remain bounded and the input error e_u converges to zero.

PROOF. See Appendix A. □

Parameter convergence is obtained if the following persistence of excitation condition [32,3,23] on the regressor matrix Φ_p is fulfilled

Definition 1 *A matrix $\Phi_p : \mathbb{R}^n \to \mathbb{R}^{p\times n}$ is persistently exciting (PE) [3] if there exist $\beta_1, \beta_2, T > 0$ such that for all $t \geq 0$ the next relationship is fulfilled*

$$\beta_1 I \leq L_1 = \int_t^{t+T} \Phi_p(\sigma)\Phi_p^\top(\sigma)d\sigma \leq \beta_2 I \tag{28}$$

The above definition requires that the $p \times p$ matrix $\Phi_p(t)\Phi_p^\top(t)$ integrated over the interval $[t, t+T]$ for all t be nonsingular, i.e the eigenvalues of the resulting matrix are different from zero.

3.2 Estimation error

It is well known that any identifier exhibits estimation errors due to unmodelled dynamics and disturbances such as noise measurements, time-delays, nonlinear disturbances in the DC motor, etc. In order to take into account these issues the closed-loop error dynamics (24) are rewritten as

$$\ddot{e} = -\bar{A}\dot{e} - \bar{B}e + \Phi_p^\top \widetilde{\Theta} + \varepsilon \tag{29}$$

where $\varepsilon = \Phi^\top \Theta - \Phi_p^\top \widehat{\Theta} \in \mathbb{R}^n$ is a bounded estimation error with $\|\varepsilon\| \leq \bar{\varepsilon}$.

Remark 2 *The estimation error ε is independent from the disturbance vector D since it depends on measurement noise and time-varying disturbances that cannot be estimated by the CLIE algorithm.*

To prove boundedness of e, $\dot{e}$ and $\widetilde{\Theta}$, the PE condition (28) and the next lemma on Linear Time Varying (LTV) systems are required.

Lemma 1 *[16] Consider the linear time-varying system defined by*

$$\begin{aligned} \dot{x}(t) &= B(t)u(t) \\ y(t) &= C(t)x(t) \end{aligned} \tag{30}$$

with $x(t) \in \mathbb{R}^n$, $u(t) \in \mathbb{R}^m$, $y(t) \in \mathbb{R}^p$ and the elements of $B(t)$ and $C(t)$ are piecewise continuous functions of time. Its Observability Grammian is

$$N(t, t+T) = \int_t^{t+T} C^\top(\sigma)C(\sigma)d\sigma.$$

Let the system (30) be uniformly completely observable (UCO) with $B(t)$ bounded. Then if $u(t)$ and $y(t)$ are bounded, then the state $x(t)$ is bounded.

Note that the PE condition (28) is equivalent to the uniform complete observability (UCO) [16] with $C(t) = \Phi_p^\top$.

The following theorem establishes the uniform ultimate boundedness (UUB) [14] of the trajectories of the system (29) and boundedness of the parameter estimates $\widehat{\Theta}$ as long as the PE condition is satisfied.

Theorem 2 *Consider the closed-loop error dynamics (29). The parameters $\widehat{\Theta}$ are updated by (27) and the regressor matrix Φ_p fulfils the PE condition (28). Define the following terms*

$$\begin{aligned} k_1 &= \min\{\lambda_{\min}(K_d\bar{B}),\ \lambda_{\min}(K_d\bar{K})\} \\ k_2 &= \max\{\lambda_{\max}(K_d),\ \lambda_{\max}(K_d K_p^{-1} K_d)\}. \end{aligned}$$

with $\bar{K} = K_p^{-1}K_d\bar{A} - I > 0$. Assume that the bound k_1 satisfies

$$k_1 > \sqrt{2}k_2\bar{\varepsilon} + \rho \tag{31}$$

where $\rho \in \mathbb{R}^+$. Then the trajectories of (29) are UUB with a practical bound given by $\mu_1 = \frac{\sqrt{2}k_2\bar{\varepsilon}}{k_1}$, and the parameter estimates $\widehat{\Theta}$ remain bounded.

PROOF. See Appendix A. □

4 Closed loop input error (CLIE) identification technique: Composite update rule

The update rule (27) can be modified by adding a second term that is a function of the identification error, which will be defined later. This approach is presented in [36] for adaptive control purposes. Here this idea is exploited for parameter identification.

4.1 Gradient method (GM)

Consider the exact model matching case, i.e., $\varepsilon = 0$. Recall the robot dynamics (9). The Laplace transform of the robot dynamics (9) is

$$Q(s) = (s^2 I + As)^{-1} \left[BU(s) - D(s)\right] \tag{32}$$

where $\mathcal{L}\{q\} = Q(s)$, $\mathcal{L}\{u\} = U(s)$ and $\mathcal{L}\{D\} = D(s)$. $\mathcal{L}(\cdot)$ denotes the Laplace transform. Model (32) is filtered by multiplying both sides of (32) by $G_2(s) = ((s+f)I)^{-1} f$

$$\begin{aligned}((s+f)I)^{-1} f Q(s) =& (s^2 I + As)^{-1}((s+f)I)^{-1} f \\ & \times \left[BU(s) - D(s)\right]\end{aligned} \tag{33}$$

The term $G_2(s)$ corresponds to the transfer function of a low-pass filter with cut-off frequency f. Note that D is a constant vector then $D(s) = \frac{1}{s} D$. Define

$$\begin{aligned} Q_f(s) &= ((s+f)I)^{-1} f Q(s) \\ sQ_f(s) &= ((s+f)I)^{-1} f sQ(s) \\ s^2 Q_f(s) &= ((s+f)I)^{-1} f s^2 Q(s) \\ U_f(s) &= ((s+f)I)^{-1} f U(s) \\ F(s) &= ((s+f)I)^{-1} f D(s) \end{aligned} \tag{34}$$

Therefore, the new filtered robot dynamics is

$$\begin{aligned} y_f \equiv \ddot{q}_f &= -A\dot{q}_f + Bu_f - F \\ &= -\Phi_f^\top \Theta \end{aligned} \tag{35}$$

where $\dot{q}_f = \mathcal{L}^{-1}\{sQ_f(s)\}$, $u_f = \mathcal{L}^{-1}\{U_f(s)\}$ and $F = \mathcal{L}^{-1}\{F(s)\}$. $\mathcal{L}^{-1}(\cdot)$ denotes the inverse Laplace transform. Here $\Phi_f = \Phi_f(q_f, \dot{q}_f, u_f)$ is given by

$$\Phi_f = \begin{bmatrix} \operatorname{diag}\left(\dot{q}_{f_i}\right)_{i=1}^n \\ -\operatorname{diag}\left(u_{f_i}\right)_{i=1}^n \\ (1 - \exp^{-ft}) I \end{bmatrix} \tag{36}$$

The filtered robot dynamics (35) eliminates measurements of the acceleration vector $\ddot{q}$, which are not available from measurements. The unknown parameters Θ in (35) can be estimated using the following model

$$\widehat{y}_f \equiv -\Phi_f^\top \widehat{\Theta} = -\widehat{A}\dot{q}_f + \widehat{B}u_f - \widehat{F} \tag{37}$$

where $\widehat{F} = (1 - \exp^{-ft})\widehat{D}$. Define the identification error

$$\epsilon = \widehat{y}_f - y_f = -\Phi_f^\top \widetilde{\Theta}. \tag{38}$$

The goal is to minimize ϵ according to the following cost index

$$J = \frac{1}{2}\epsilon^\top \epsilon$$

subject to (35) and (37).

The GM update rule is defined as

$$\dot{\widehat{\Theta}} = -\alpha \frac{\partial J}{\partial \widehat{\Theta}} = \alpha \Phi_f \epsilon \tag{39}$$

with $\alpha \in \mathbb{R}^+$, and it is added to (27) to improve parameter convergence. The resulting composite update rule is

$$\dot{\widehat{\Theta}} = -\Gamma \Phi_p K_d K_p^{-1} e_u + \alpha \Gamma \Phi_f \epsilon. \tag{40}$$

The first term of the right-hand side of (40) would guarantee stability and boundedness of the parameters estimates, whereas the second term of the right-hand-side of (40) would improve the parameters convergence if the PE signal is rich enough.

Moreover, the update rule (40) is written as an LTV system of the form

$$\begin{aligned} \dot{\widetilde{\Theta}} &= \Gamma \Phi_p K_d K_p^{-1} u_1 + \alpha \Gamma \Phi_f u_2 \\ y &= \Phi_p^\top \widetilde{\Theta} \\ z &= \Phi_f^\top \widetilde{\Theta} = -\epsilon, \end{aligned} \tag{41}$$

where y and z are the system outputs. The above system corresponds to a feedback interconnection with input $u_1 = -e_u$ and feedback signal $u_2 = -z$.

It is assumed that matrix Φ_f fulfils the next PE condition

Definition 2 *The matrix $\Phi_f : \mathbb{R}^n \to \mathbb{R}^{p \times n}$ is persistently exciting (PE) [3] if there exist $\beta_{f_1}, \beta_{f_2}, T > 0$ such that for all $t \geq 0$ the next inequality holds*

$$\beta_{f_1} I \leq L_f = \int_t^{t+T} \Phi_f(\sigma)\Phi_f^\top(\sigma) d\sigma \leq \beta_{f_2} I \tag{42}$$

On the other hand, assume that the error e_u is zero in (40), which yields

$$\dot{\widetilde{\Theta}} = -\alpha \Gamma \Phi_f \Phi_f^\top \widetilde{\Theta}. \tag{43}$$

Therefore, the solution of (43) is

$$\widetilde{\Theta}(t) = \widetilde{\Theta}(0) \exp^{-\alpha \Gamma \int_0^t \Phi_f(\sigma)\Phi_f^\top(\sigma) d\sigma} \tag{44}$$

and $\widetilde{\Theta}$ converges exponentially to zero if Φ_f satisfies the PE condition (42). The exponential convergence proof is similar to what is presented in Theorem 2.5.3 of [33].

The next result shows the exponential stability of the error dynamics (24) under the update rule (40).

Theorem 3 *Consider the error dynamics (24). Let the parameter estimates $\widehat{\Theta}$ be generated by the update rule (40), $K_p^{-1}K_d\bar{A} - I > 0$ and the regressors Φ_p and Φ_f fulfil the PE conditions (28) and (42), respectively. Then the parameter error $\widetilde{\Theta}$ converges exponentially to zero.*

PROOF. See Appendix A. □

4.2 Estimation error

In this section the performance of the CLIE technique is analyzed based on the composite update rule (40) in presence of estimation errors.

The identification error ϵ may be affected by an estimation error due to unmodelled dynamics and disturbances. To consider this issue, the equation (38) is rewritten as

$$\epsilon = \widehat{y}_f - y_f = -\Phi_f^\top \widetilde{\Theta} + \varsigma, \tag{45}$$

where $\varsigma \in \mathbb{R}^n$ is a bounded estimation error with $\|\varsigma\| \leq \bar{\varsigma}$. This error may introduces biases in the parameters estimates $\widehat{\Theta}$, which in turn may influence the tracking error e. Note also that the estimation error ε may also affect e.

The next results establishes the UUB of the trajectories of the system (29) and boundedness of the parameter estimates $\widehat{\Theta}$ as long as the PE conditions (28) and (42) are satisfied.

Theorem 4 *Consider the closed-loop error dynamics (29). The parameter estimates $\widehat{\Theta}$ are updated by (40) and the regressors Φ_p and Φ_f fulfill the PE conditions (28) and (42), respectively. Define the following terms*

$$k_3 = \max\{\min\{\lambda_{\min}(K_d\bar{B}), \lambda_{\min}(K_d\bar{K})\}, \alpha\}$$
$$k_4 = \max\{\lambda_{\max}(K_d), \lambda_{\max}(K_dK_p^{-1}K_d), \alpha\}$$

with $\bar{K} = K_p^{-1}K_d\bar{A} - I > 0$. Assume that the bound k_3 satisfies

$$k_3 > \sqrt{2\bar{\varepsilon}^2 + \bar{\varsigma}^2}k_4 + \varrho \tag{46}$$

where $\varrho \in \mathbb{R}^+$. Then the trajectories of (29) are UUB with a practical bound given by $\mu_2 = \frac{\sqrt{2\bar{\varsigma}+\bar{\varepsilon}}k_4}{k_3}$, and the parameter estimates $\widehat{\Theta}$ remain bounded.

PROOF. See Appendix A. □

Note that the GM in the composite update law helps improving the negativity of the time derivative of $\dot{V}$ and to ensure exponential convergence of the parameter estimates. However, it introduces an estimation error ς producing a bias in the parameter estimates $\widehat{\Theta}$.

5 Numerical simulation studies

The performance of the CLIE and CLIE+GM identification algorithms are assessed using a 2-DOF robot model actuated by DC motors endowed with a gearbox.

The dynamics (1) of the 2-DOF robot (without friction)[13] is

$$M(q) = \begin{bmatrix} (m_1+m_2)l_1^2 + w_1 + 2w_2 + J_1 & w_1 + w_2 \\ w_1 + w_2 & w_1 \end{bmatrix}$$
$$C(q,\dot{q}) = \begin{bmatrix} \frac{\partial w_2}{\partial q_2}\dot{q}_2 & \frac{\partial w_2}{\partial q_2}(\dot{q}_1 + \dot{q}_2) \\ -\frac{\partial w_2}{\partial q_2}\dot{q}_1 & 0 \end{bmatrix}$$
$$G(q) = \begin{bmatrix} (m_1+m_2)gl_1\cos(q_1) + w_3 \\ w_3 \end{bmatrix}$$

where q_1 and q_2 define the joint angles of the 2-DOF robot, m_k, J_k and l_k stand for the mass, inertia and length of each link $k = 1, 2$, $g = 9.81$ m/s^2 is the gravity acceleration and $w_1 = m_2l_2^2 + J_2$, $w_2 = m_2l_1l_2\cos(q_2)$, $w_3 = m_2gl_2\cos(q_1+q_2)$. The robot parameters are $m_1 = m_2 = 0.5$ kg and $l_1 = l_2 = 0.6$ m. The Simulink diagrams use a sampling period of 0.1ms and the ODE5 solver to obtain more accurate approximations of the continuous-time update laws and the filters employed in the simulations. Gaussian noise $\Delta q \sim \mathcal{N}(0, \sigma^2)$ of small magnitude is used to model position measurement noise. The Gaussian noise is obtained from the *random number* block of Simulink with a variance of $\sigma^2 = 1 \times 10^{-3}$ and a mean $\mu = 0$. The following transfer function composed by a high-pass filter in cascade with low-pass filter was used to obtain velocity estimates from position measurements

$$G_1(s) = \frac{200s}{s+200}\frac{300}{s+300}\begin{bmatrix} 1 & 0 \\ 0 & 1 \end{bmatrix} \in \mathbb{C}^{2\times 2}. \tag{47}$$

The cut-off frequency of the high and low-pass filter were selected manually such that the high frequency components of the position measurements were attenuated.

Each DC motor dynamics (4) driving the robot links has the following parameters: $J_k = 1/50$ kgm^2 and $R_k = 1/25$ kgm^2/s. The gear ratio r_k=100.

The interaction between the robot dynamics (1), the DC motor dynamics (4) and the gearbox relation (5) gives the decoupled dynamics, which in the case of the 2-DOF robot is

$$\begin{aligned}\begin{bmatrix}\ddot{q}_1\\ \ddot{q}_2\end{bmatrix} &= -\begin{bmatrix}A_1 & 0\\ 0 & A_2\end{bmatrix}\begin{bmatrix}\dot{q}_1\\ \dot{q}_2\end{bmatrix} + \begin{bmatrix}B_1 & 0\\ 0 & B_2\end{bmatrix}\begin{bmatrix}u_1\\ u_2\end{bmatrix} - \begin{bmatrix}D_1\\ D_2\end{bmatrix}\\ &= -\Phi^\top\Theta\end{aligned}$$

where A_k, B_k and D_k are the robot parameters. The regressor matrix Φ and the parameters vector Θ are

$$\begin{aligned}\Phi &= \begin{bmatrix}\dot{q}_1 & 0 & -u_1 & 0 & 1 & 0\\ 0 & \dot{q}_2 & 0 & -u_2 & 0 & 1\end{bmatrix}^\top\\ \Theta &= \begin{bmatrix}A_1 & A_2 & B_1 & B_2 & D_1 & D_2\end{bmatrix}^\top.\end{aligned}$$

Hence, the identification algorithms estimate six parameters. In contrast to the CLOE method, the CLIE method does not require to initialize the parameters estimates using previous values obtained under open loop conditions or from CAD blueprints [6,7]. For this simulation study the parameter estimates and the robot initial conditions are initialized at zero.

5.1 System identification

The estimated model for the 2-DOF robot is

$$\begin{aligned}\begin{bmatrix}\ddot{p}_1\\ \ddot{p}_2\end{bmatrix} &= -\begin{bmatrix}\widehat{A}_1 & 0\\ 0 & \widehat{A}_2\end{bmatrix}\begin{bmatrix}\dot{p}_1\\ \dot{p}_2\end{bmatrix} + \begin{bmatrix}\widehat{B}_1 & 0\\ 0 & \widehat{B}_2\end{bmatrix}\begin{bmatrix}v_1\\ v_2\end{bmatrix} - \begin{bmatrix}\widehat{D}_1\\ \widehat{D}_2\end{bmatrix}\\ &= -\Phi_p^\top\widehat{\Theta}\end{aligned}$$

$\widehat{A}_k$, $\widehat{B}_k$ and $\widehat{D}_k$ are the estimates of the robot parameters. The regressor Φ_p, and the parameter estimates $\widehat{\Theta}$ are

$$\begin{aligned}\Phi_p &= \begin{bmatrix}\dot{p}_1 & 0 & -v_1 & 0 & 1 & 0\\ 0 & \dot{p}_2 & 0 & -v_2 & 0 & 1\end{bmatrix}^\top\\ \widehat{\Theta} &= \begin{bmatrix}\widehat{A}_1 & \widehat{A}_2 & \widehat{B}_1 & \widehat{B}_2 & \widehat{D}_1 & \widehat{D}_2\end{bmatrix}^\top.\end{aligned}$$

For the composite update rule (40) the next filter is used to avoid acceleration measurements

$$G_2(s) = \frac{300}{s+300}\begin{bmatrix}1 & 0\\ 0 & 1\end{bmatrix} \in \mathbb{C}^{2\times 2}.$$

The above filter is tuned manually to reduce the high-frequency components of the position measurements. The filtered dynamics (37) is:

$$\begin{aligned}\begin{bmatrix}\ddot{q}_{f_1}\\ \ddot{q}_{f_2}\end{bmatrix} &= -\begin{bmatrix}\widehat{A}_1 & 0\\ 0 & \widehat{A}_2\end{bmatrix}\begin{bmatrix}\dot{q}_{f_1}\\ \dot{q}_{f_2}\end{bmatrix} + \begin{bmatrix}\widehat{B}_1 & 0\\ 0 & \widehat{B}_2\end{bmatrix}\begin{bmatrix}u_{f_1}\\ u_{f_2}\end{bmatrix} - \begin{bmatrix}\widehat{D}_1\\ \widehat{D}_2\end{bmatrix}\\ &= -\Phi_f^\top\widehat{\Theta}\end{aligned}$$

and the regressor Φ_f is given by

$$\Phi_f = \begin{bmatrix}\dot{q}_{f_1} & 0 & -u_{f_1} & 0 & 1-e^{-300t} & 0\\ 0 & \dot{q}_{f_2} & 0 & -u_{f_2} & 0 & 1-e^{-300t}\end{bmatrix}^\top.$$

The following PE signal is chosen using low frequency sine waves and their amplitudes and frequencies are set by a trial and error procedure.

$$PE = 0.7\sin(2\pi t) + 0.5\sin(\pi t) - 0.25\cos(\pi t) \quad (48)$$

In practice other factors should be considered for designing a PE signal. It must be smooth to avoid sudden velocity changes in the robot that could affect its mechanical integrity. The amplitude of the PE signal should be chosen such that the robot joints do not reach its mechanical limits, and the power amplifiers do not saturate or reach its maximum current limits. Moreover, the bandwidth of the PE signal should produce joint velocities respecting their maximum allowable values.

On the other hand, condition (28) in Definition 1 cannot be established in practice because it requires verifying the positive definiteness of the integral of the matrix $\Phi\Phi^\top$ in a time window $[t, t+T]$ for all time t. However, it is possible to evaluate the condition in a finite number of windows to verify that at least the PE condition holds in these time instants. To this end, consider the following weighted scalar PE condition

$$\beta_{w_1} \leq \int_t^{t+T} w^\top\Phi_p(\sigma)\Phi_p^\top(\sigma)w d\sigma \leq \beta_{w_2}, \quad (49)$$

where $w = \frac{1}{\sqrt{p}}\vec{1}_p$, $\vec{1}_p = \begin{bmatrix}1 & \dots & 1\end{bmatrix}^\top \in \mathbb{R}^p$, and β_{w_1},β_{w_2}, $T > 0$. The values of Φ_p used for computing (49) are the ones obtained from the simulation corresponding to the CASE 1 in Table 1. Notice that the PE condition (49) is a scalar value instead of a $p \times p$ matrix as in (28), then, computing and visualizing condition (49) is easier. For this study $p = 6$ and the time window is $T = 10$ s except for the first window. Fig. 3 shows the time-evolution of the weighted PE signal condition at time windows starting at 0,5,15,25,35 and 45 s. At the end of each time window the integral is reset.

It is easy to check that in all the cases the value of the integral (49), which corresponds to the peaks in the graph,

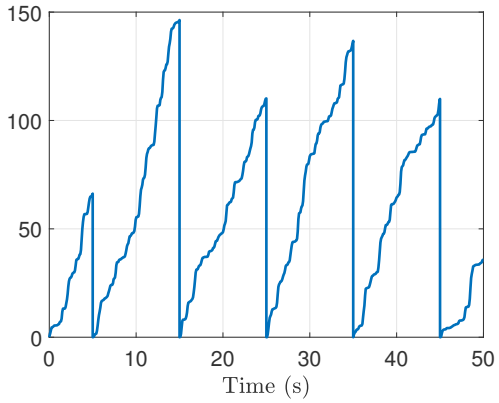

Fig. 3. Weighted PE condition plot

is always positive. Therefore, the proposed PE signal satisfies (49) and consequently (28) at least at the these time windows. A similar procedure can be done to verify the PE condition (42).

The gains of the PD controller were tuned off-line through a manual procedure without using the PE signal and applying step responses. The tuning starts by setting to zero the K_p gains and setting the K_d gains to non-zero low values. Then, increase the K_p until overshoots appear, then increase K_d to add damping until the oscillations disappear. Increase again K_p and then K_d. The goal is to set the K_p as high as possible while obtaining a nonovershooting response.

The final gains were set to $K_p = 10I$ and $K_d = 5I$. These gains were tested to verify (18) using the real values of Table 2 and the PE signal (48). For the proposed signal the disturbance vector was bounded by $\|\eta\| = \|BPE - D\| = 0.8768$. The closed-loop trajectories of (12) converged to a compact set S_x with radius $\mu_0 = 0.9637$ which verifies the UUB stability of the closed-loop trajectories of the robot under the PD control law. Furthermore, it is possible to verify that μ_0 increases or decreases when the PD gains are decreased or increased, that is, if the gains are decreased to $K_p = 8I$ and $K_d = 4I$ then the radius μ_0 increases to $\mu_0 = 0.9845$. On the other hand, if the gains are increased to $K_p = 12I$ and $K_d = 6I$ then $\mu_0 = 0.9485$.

Three different composite update identification experiments are executed. CASE 1 corresponds to the CLIE update law (27) whereas CASE 2 and CASE 3 considers the update law (40). The gains in each case are given in Table 1.

Fig. 4 shows the time evolution of the parameter estimates. Table 2 summarizes the mean value of the parameters estimates and the parametric error percentage obtained as $|\widetilde{\Theta}_k| \times 100\%$, of each identification algorithm during the last 20 seconds.

Table 1
Gains for the update rules (27) and (40)

CASE	**Γ gain**	**GM Gain α**
CASE 1 update law (27)	$20I$	-
CASE 2 update law (40)	$20I$	0.0001
CASE 3 update law (40)	$20I$	0.001

The results of Table 2 and Fig. 4 show that the composite rule in CASE 2 improves parameter convergence and presents less parametric error percentage in comparison to CASE 3. The main difference between CASE 2 and CASE 3 is that large values of the update gain α increase the effect of the estimation error ζ. On the other hand, small values of Γ causes slow convergence of the CLIE algorithm (27). Therefore, the gain Γ has to be selected large enough to ensure fast estimates convergence, and the update gain α has to be selected small enough, but not zero, to ensure that the estimation error ε is small. It is worth mentioning that the gain values depends on the selection of the PE signal and using other excitation signal may required changing the gain values.

The disturbance estimates $\widehat{D}_1$ and $\widehat{D}_2$ have different values for each identification method due to the incorporation of the filtered dynamics in the update law. The filtered dynamics has small amounts of noise attributed to the Gaussian noise Δq.

The estimates of Table 2 are used to compute the estimation error $\varepsilon = \Phi_p^\top \widehat{\Theta} - \Phi^\top \Theta = [\varepsilon_1, \varepsilon_2]^\top$ of each identification method for 100 seconds of simulation time. The mean estimation error $\bar{\varepsilon}_k = \frac{1}{100} \sum_{t=0}^{100} \varepsilon_k(t)$ is used to obtain the mean value of the estimation error, with $k = 1, 2$. Notice that $\bar{\varepsilon}_k$ denote the mean estimation error of the DOF k, and $\bar{\varepsilon}$ denotes an upper bound of $\|\varepsilon\|$. The numerical results are given in Table 3.

The mean error results shows that the CASE 1 has better performance in comparison to the CASE 3. The main reason is because the composite rule adds the estimation error ς which increases when a large gain α is used. Both CASE 1 and CASE 2 methods have similar mean estimation error $\bar{\varepsilon}_k$.

The estimation error norm $\|\varepsilon\| = \sqrt{\sum_{k=1}^{2} \bar{\varepsilon}_k^2}$ is used to validate the condition (31) and (46). The estimation error norm for each case are $\|\varepsilon\|_{CASE\ 1} = 2.36 \times 10^{-5}$, $\|\varepsilon\|_{CASE\ 2} = 2.3 \times 10^{-5}$ and $\|\varepsilon\|_{CASE\ 3} = 8.86 \times 10^{-5}$. The following terms are obtained by considering knowledge of the real parameters: $k_1 = 11.19$, $k_2 = 5$, $k_3 = 11.19$, $k_4 = 5$. The estimation error $\bar{\zeta}$ is assumed

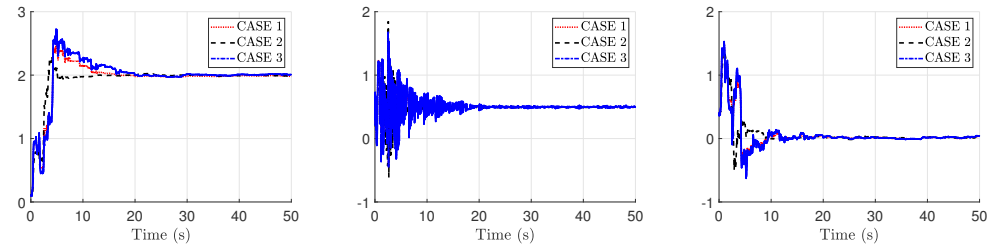

(a) Parameter estimate $\widehat{A}_1$ (b) Parameter estimate $\widehat{B}_1$ (c) Parameter estimate $\widehat{D}_1$

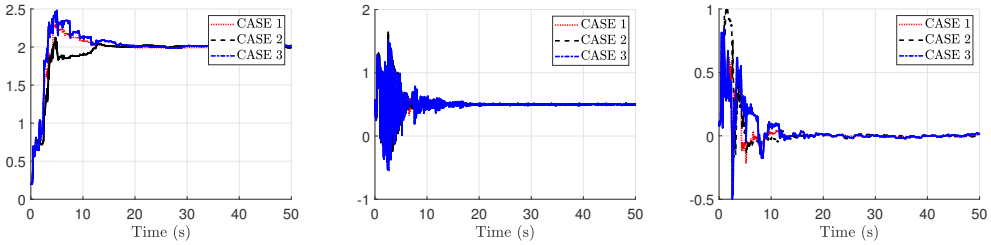

(d) Parameter estimate $\widehat{A}_2$ (e) Parameter estimate $\widehat{B}_2$ (f) Parameter estimate $\widehat{D}_2$

Fig. 4. Parameter estimates of the 2-DOF planar robot

Table 2
Parameter estimates of the 2-DOF planar robot through the composite update rule (40)

	Approximate	**CLIE Algorithm**					
Estimate $\widehat{\Theta}_k$	**Real value** Θ_k	**CASE 1**	**CASE 1** $\lvert\widetilde{\Theta}_k\rvert$ **(%)**	**CASE 2**	**CASE 2** $\lvert\widetilde{\Theta}_k\rvert$ **(%)**	**CASE 3**	**CASE 3** $\lvert\widetilde{\Theta}_k\rvert$ **(%)**
$\widehat{A}_1$	1.9891	1.9839	0.52	1.9855	0.36	2.0015	1.24
$\widehat{A}_2$	1.9952	1.9926	0.26	1.9943	0.09	2.0103	1.51
$\widehat{B}_1$	0.4973	0.4964	0.09	0.4964	0.09	0.4968	0.05
$\widehat{B}_2$	0.4998	0.4983	0.19	0.4983	0.15	0.4985	0.13
$\widehat{D}_1$	0.0113	0.0132	0.05	0.0129	0.16	0.0098	0.15
$\widehat{D}_2$	-0.0026	-0.0018	0.08	-0.0021	0.05	-0.005	0.24

to be equivalent to $\bar{\varepsilon}$. Then,

$$k_1 > \sqrt{2}k_2\bar{\varepsilon} = 1.67 \times 10^{-4}$$
$$k_3 > \sqrt{2\bar{\varepsilon}^2_{CASE\ 2} + \bar{\zeta}^2}, \quad k_4 = 1.99 \times 10^{-4}$$
$$k_3 > \sqrt{2\bar{\varepsilon}^2_{CASE\ 3} + \bar{\zeta}^2}, \quad k_4 = 7.67 \times 10^{-4}$$

The above inequalities are satisfied according to the obtained values for k_1 and k_3. Furthermore, it is easy to check that the scalars ρ and ϱ of each case are equal to: $\rho \cong \varrho_{CASE\ 2} \cong \varrho_{CASE\ 3} = 11.19$.

5.2 Validation

The parameter estimates of Table 2 are validated by computing the feedback linearization controller depicted in Fig. 5. The diagram is composed of four main components: a desired joint position reference q_d; a PD control law designed as in Fig. 2; a dynamic compensation which uses the estimates obtained from the CLIE cases; and the robot manipulator which in this case is a 2-DOF robot.

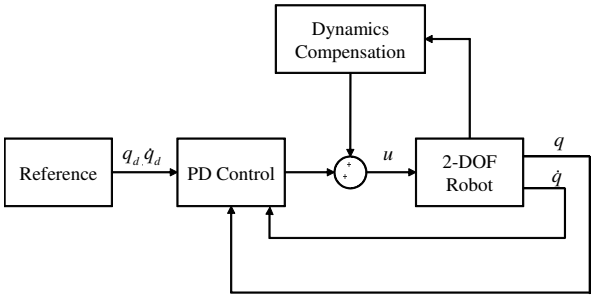

Fig. 5. Feedback linearization controller scheme.

The feedback linearization controller is

$$u = \widehat{B}^{-1}\left[\widehat{A}\dot{q} - \widehat{D} + K_p\widetilde{q} + K_d\dot{\widetilde{q}} + \ddot{q}_d\right] \tag{50}$$

where same K_p and K_d gains of the previous identification experiment are employed; $q_d, \dot{q}_d, \ddot{q}_d$ are the desired joint position, velocity and acceleration, respectively. $\widetilde{q} = q_d - q$ and $\dot{\widetilde{q}} = \dot{q}_d - \dot{q}$ are the position and velocity

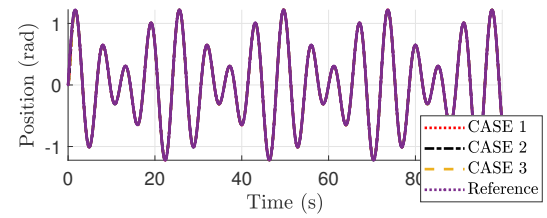

(a) Position tracking of joint q_1

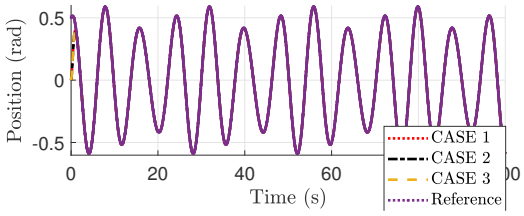

(b) Position tracking of joint q_2

Fig. 6. Tracking control results of the 2-DOF robot

tracking errors, respectively. The desired reference is

$$q_d = \begin{bmatrix} \frac{1}{2}\sin\left(\frac{\pi}{4}t\right) + \frac{3}{4}\sin\left(\frac{\pi}{3}t\right) \\ \frac{1}{10}\sin\left(\frac{\pi}{3}t\right) + \frac{1}{2}\cos\left(\frac{\pi}{4}t\right) \end{bmatrix}.$$

The feedback linearization controllers compensate the dynamics of the 2-DOF robot and establish a desired dynamic behaviour given by the PD control law.

Fig. 6 shows the tracking results using the estimates of Table 2 and the feedback linearization controller (50). The results show an accurate tracking performance for each identification method, which means that the parameter estimates $\widehat{\Theta}$ are close to their real values Θ.

The mean squared error $\overline{q}_k = \frac{1}{100}\sum_{t=0}^{100} \widetilde{q}_k^2(t)$ of the tracking error $\widetilde{q}$ is used to show the accuracy of the feedback linearization controller under the estimates of Table 2. The numerical results of the estimation error $\|\varepsilon\|$ and the mean squared tracking and estimation errors $\bar{q}_k$ and $\bar{\varepsilon}_k$ are summarized in Table 3.

These outcomes show that the proposed approach obtains reliable estimates that are closer to their real values. Furthermore, the composite rule adds another estimation error due to the filtered dynamics that cannot be compensated using the proposed approach, which is a topic of future work.

6 Conclusion

This work exposes a Closed Loop Input Error (CLIE) method for an on-line identification of robot manipulators. The advantage of this method is that it depends on a PD controller whose gains are freely chosen such that they only need to stabilize the robot dynamics. Moreover, the regressor used in the method does not depend on noisy measurements and uses only the the noise-free states of an estimated model. A composite update rule based on a gradient method that improves parameter convergence is also proposed. Stability and convergence of the proposed approach is assessed using Lyapunov stability theory, which takes into account the Persistency of Exciting conditions. Numerical simulations are carried out to support the proposed approach.

Regarding future work, inverse control problem [1] has become popular in recent years in human-behavior learning applications in order to extract useful features of a given control law, such as the weight matrices of a cost function or an approximation and parametrization of an utility function [25]. Since the control input is known and stabilizes the closed-loop system, then a modified CLIE method could be used to solve the inverse control problem.

Another issue worth studying is how to attenuate or even eliminate the bias introduced by the Gradient Method in the composite update law (40) fed by the identification error ϵ. A way to circumvent this problem is to assume a model of the estimation error ς in (45) expressed as a linear regression containing known functions and unknown parameters. For instance, the model could be a sum of sinusoids each having unknown amplitude and phase. Then, the estimation of the unknown parameters could be carried out together with the robot parameters.

A Proofs

Proof of Theorem 1. Consider the next Lyapunov function

$$\begin{aligned} V =& \frac{1}{2} e_u^\top K_p^{-1} e_u + \frac{1}{2}\widetilde{\Theta}^\top \Gamma^{-1}\widetilde{\Theta} \\ &+ \frac{1}{2} e^\top \left[\bar{B}^\top K_d K_p^{-1} K_d + K_p\left(K_p^{-1} K_d \bar{A} - I\right)\right] e \end{aligned} \tag{A.1}$$

This function is positive definite if $K_p^{-1}K_d\bar{A} - I > 0$. Recall that $\bar{A}$, $\bar{B}$, Γ, K_p and K_d are diagonal matrices since the system is decoupled. The time-derivative of (A.1) is

$$\begin{aligned} \dot{V} =& e_u^\top K_p^{-1}\left(K_p\dot{e} + K_d\ddot{e}\right) + \widetilde{\Theta}^\top\Gamma^{-1}\dot{\widetilde{\Theta}} \\ &+ e^\top\left(K_d\bar{A} + \bar{B}^\top K_d K_p^{-1} K_d - K_p\right)\dot{e} \\ =& - e^\top K_d \bar{B} e - \dot{e}^\top K_d (K_p^{-1}K_d\bar{A} - I)\dot{e} \\ &+ \widetilde{\Theta}^\top(\Gamma^{-1}\dot{\widetilde{\Theta}} + \Phi_p K_d K_p^{-1} e_u) \end{aligned}$$

Table 3
Estimation and mean squared tracking errors numerical values.

CLIE	$\bar{\varepsilon}_1$	$\bar{\varepsilon}_2$	$\|\varepsilon\|$	$\bar{q}_1$	$\bar{q}_2$
CASE 1	2.29×10^{-5}	5.54×10^{-6}	2.39×10^{-5}	1.468×10^{-7}	9.342×10^{-7}
CASE 2	2.23×10^{-5}	5.66×10^{-6}	2.3×10^{-5}	1.468×10^{-7}	9.342×10^{-7}
CASE 3	6.26×10^{-5}	6.26×10^{-5}	8.86×10^{-5}	1.481×10^{-7}	9.342×10^{-7}

If the update law is chosen as (27), then the time-derivative of the Lyapunov function simplifies to

$$\begin{aligned}\dot{V} &= -e^\top K_d\bar{B}e - \dot{e}^\top K_d(K_p^{-1}K_d\bar{A} - I)\dot{e} \\ &= -\begin{bmatrix} e \\ \dot{e}\end{bmatrix}^\top \underbrace{\begin{bmatrix} K_d\bar{B} & 0 \\ 0 & K_d(K_p^{-1}K_d\bar{A} - I)\end{bmatrix}}_{Q\in\mathbb{R}^{2n\times 2n}} \begin{bmatrix} e \\ \dot{e}\end{bmatrix} \\ &\leq -\lambda_{\min}(Q)\|E\|^2 \end{aligned} \tag{A.2}$$

where $E = [e^\top, \dot{e}^\top]^\top$. The matrix Q is positive definite if $K_p^{-1}K_d\bar{A} - I > 0$. From (A.2), it is clear that E is an $\mathcal{L}_\infty$ function and $V(0) \geq V$. On the other hand, boundedness of E implies boundedness of p and $\dot{p}$; hence, the control input v and the regressor vector Φ_p are also bounded. In summary $E, p, \dot{p}, v, \Phi_p \in \mathcal{L}_\infty$.

Barbalat's lemma can be applied to prove the convergence of E and e_u to zero. Integrating (A.2) yields

$$V(t) - V(0) \leq -\int_0^t \lambda_{\min}(Q)\|E\|^2 d\tau.$$

The next inequality follows from this last result

$$\int_0^t \|E\|^2 d\tau \leq \frac{V(0)}{\lambda_{\min}(Q)} < \infty. \tag{A.3}$$

From (A.3), it follows that E is an $\mathcal{L}_2$ function. Boundedness of the parametric error $\widetilde{\Theta}$, e and $\dot{e}$ in (A.2) allow concluding that $\dot{E} = [\dot{e}^\top, \ddot{e}^\top]^\top$ is an $\mathcal{L}_\infty$ function. Applying Barbalat's lemma permits concluding that E converges to zero. Finally, from (26) it is clear that e_u converges to zero. □

Proof of Theorem 2. Consider again the Lyapunov function (A.1). Its time derivative along the identification error dynamics (29) is

$$\begin{aligned}\dot{V} =& e_u^\top K_p^{-1}\left(K_p\dot{e} + K_d\ddot{e}\right) + \widetilde{\Theta}^\top\Gamma^{-1}\dot{\widetilde{\Theta}} \\ &+ e^\top\left(K_d\bar{A} + \bar{B}^\top K_d K_p^{-1}K_d - K_p\right)\dot{e} \\ =& -e^\top K_d\bar{B}e - \dot{e}^\top K_d(K_p^{-1}K_d\bar{A} - I)\dot{e} \\ &+ \widetilde{\Theta}^\top(\Gamma^{-1}\dot{\widetilde{\Theta}} + \Phi_p K_d K_p^{-1}e_u) + e_u^\top K_p^{-1}K_d\varepsilon\end{aligned}$$

If the update law is chosen as (27), then the time-derivative of the Lyapunov function simplifies to

$$\begin{aligned}\dot{V} =& -e^\top K_d\bar{B}e - \dot{e}^\top K_d(K_p^{-1}K_d\bar{A} - I)\dot{e} + e_u^\top K_p^{-1}K_d\varepsilon \\ =& -e^\top K_d\bar{B}e - \dot{e}^\top K_d\bar{K}\dot{e} + e^\top K_d\varepsilon + \dot{e}^\top K_d K_p^{-1}K_d\varepsilon \\ \leq& -\lambda_{\min}(K_d\bar{B})\|e\|^2 - \lambda_{\min}(K_d\bar{K})\|\dot{e}\|^2 \\ &+ \bar{\varepsilon}\lambda_{\max}(K_d)\|e\| + \bar{\varepsilon}\lambda_{\max}(K_d K_p^{-1}K_d)\|\dot{e}\| \\ \leq& -k_1\|\zeta\|^2 + \sqrt{2}k_2\bar{\varepsilon}\|\zeta\| \\ =& -k_1\|\zeta\|\left(\|\zeta\| - \frac{\sqrt{2}k_2\bar{\varepsilon}}{k_1}\right)\end{aligned} \tag{A.4}$$

where $\zeta = [\|e\|, \|\dot{e}\|]^\top$ and $\|\zeta\| = \|E\|$. Therefore $\dot{V} \leq 0$ as long as

$$\|E\| > \frac{\sqrt{2}k_2\bar{\varepsilon}}{k_1} \equiv \mu_1. \tag{A.5}$$

Selecting the control gains K_p and K_d such that (31) is satisfied ensures that the trajectories of the system (29) converge to a compact set S_E of radius μ_1, i.e., $\|E\| \leq \mu_1$ and hence, the trajectories of (29) are UUB.

Boundedness of E implies boundedness of e_u, p and $\dot{p}$; hence the control input v and the regressor Φ_p are also bounded. It can be shown that $\|\dot{E}\|$ is bounded as it is done in Theorem 1. These facts guarantee boundedness of the term

$$y \equiv \ddot{e} + \bar{A}\dot{e} + \bar{B}e - \varepsilon \tag{A.6}$$

From (29) it can be seen that the output (A.6) is equivalent to $y = \Phi^\top\widetilde{\Theta}$. The dynamics of $\widetilde{\Theta}$ can be expressed as in (30) by substituting the input error (26) as follows

$$\begin{aligned}\dot{\widetilde{\Theta}} &= -\Gamma\Phi_p K_d K_p^{-1}\begin{bmatrix} K_p & K_d\end{bmatrix}E \\ y &= \Phi_p^\top\widetilde{\Theta}\end{aligned} \tag{A.7}$$

Let $B(t) = -\Gamma\Phi_p K_d K_p^{-1}\begin{bmatrix}K_p & K_d\end{bmatrix}$, $x(t) = \widetilde{\Theta}$, $C(t) = \Phi_p^\top$ and $u(t) = E$. Since y, E and Φ_p are bounded and Φ_p is PE, so by Lemma 1 boundedness of E and y ensures boundedness of the parametric error $\widetilde{\Theta}$, and hence $\widehat{\Theta}$. □

Proof of Theorem 3. Consider the following Lyapunov function

$$\begin{aligned}V =&\frac{1}{2}e_u^\top K_p^{-1}e_u + \frac{1}{2}\widetilde{\Theta}^\top\Gamma^{-1}\widetilde{\Theta}\\ &+\frac{1}{2}e^\top\left[\bar{B}^\top K_d K_p^{-1}K_d + K_p(K_p^{-1}K_d\bar{A} - I)\right]e\end{aligned} \tag{A.8}$$

Its time derivative along the identification error dynamics (24) under the update rule (40) and considering (38) is

$$\begin{aligned}\dot{V} =& -e^\top K_d\bar{B}e - \dot{e}^\top K_d(K_p^{-1}K_d\bar{A} - I)\dot{e} - \alpha\epsilon^\top\epsilon\\ =& -E^\top QE - \alpha\epsilon^\top\epsilon\end{aligned} \tag{A.9}$$

From (A.9) it is clear that both E and $\widetilde{\Theta}$ are an $\mathcal{L}_\infty$ functions and $V(0) \geq V$ if $K_p^{-1}K_d\bar{A} - I > 0$. Note from (A.9) that

$$\begin{aligned}\dot{V} \leq& -E^\top QE\\ \leq& -\lambda_{\min}(Q)\|E\|^2.\end{aligned} \tag{A.10}$$

Applying the results of Theorem 1, the convergence to zero of E can be concluded. Moreover, the parametric error $\widetilde{\Theta}$ is bounded. Since E converges to zero then e_u also converges to zero. From (43), it can be seen that $\widetilde{\Theta}$ converges exponentially to zero by considering $e_u = 0$, then (40) represents and exponentially stable dynamics and hence the convergence of the estimated parameters $\widehat{\Theta}$ to the true parameters Θ can be concluded under a convergent input $\Phi_p K_d K_p^{-1}e_u$ to zero[35]. □

Proof of Theorem 4. The time derivative of the Lyapunov function (A.8) along the closed-loop error dynamics (29) trajectories is

$$\begin{aligned}\dot{V} =& -e^\top K_d\bar{B}e - \dot{e}^\top K_d(K_p^{-1}K_d\bar{A} - I)\dot{e} + e_u^\top K_p^{-1}K_d\varepsilon\\ &+\widetilde{\Theta}^\top(\Gamma^{-1}\dot{\widetilde{\Theta}} + \Phi_p K_d K_p^{-1}e_u)\\ =& -e^\top K_d\bar{B}e - \dot{e}^\top K_d\bar{K}\dot{e} + e^\top K_d\varepsilon + \dot{e}^\top K_d K_p^{-1}K_d\varepsilon\\ &-\alpha\widetilde{\Theta}^\top\Phi_f\left(\Phi_f^\top\widetilde{\Theta} - \varsigma\right)\\ \leq& -\lambda_{\min}(K_d\bar{B})\|e\|^2 - \lambda_{\min}(K_d\bar{K})\|\dot{e}\|^2 - \alpha\|\epsilon\|^2\\ &+\alpha\bar{\varsigma}\|\epsilon\| + \bar{\varepsilon}\lambda_{\max}(K_d)\|e\| + \bar{\varepsilon}\lambda_{\max}(K_d K_p^{-1}K_d)\|\dot{e}\|\end{aligned}$$

Define $\Sigma = [\|e\|, \|\dot{e}\|, \|\epsilon\|]^\top$, then

$$\dot{V} \leq -k_3\|\Sigma\|^2 + k_4\bar{\varepsilon}\bar{\varsigma}\Sigma^\top\Psi$$

where $\Psi = \left[\frac{1}{\bar{\varsigma}}, \frac{1}{\bar{\varsigma}}, \frac{1}{\bar{\varepsilon}}\right]^\top$. Then

$$\begin{aligned}\dot{V} \leq& -k_3\|\Sigma\|^2 + \sqrt{2\bar{\varepsilon}^2 + \bar{\varsigma}^2}k_4\|\Sigma\|\\ =& -k_3\|\Sigma\|\left(\|\Sigma\| - \frac{\sqrt{2\bar{\varepsilon}^2 + \bar{\varsigma}^2}k_4}{k_3}\right).\end{aligned} \tag{A.11}$$

Therefore $\dot{V} \leq 0$ as long as

$$\|\Sigma\| > \frac{\sqrt{2\bar{\varepsilon}^2 + \bar{\varsigma}^2}k_4}{k_3} \equiv \mu_2. \tag{A.12}$$

If (46) is satisfied, then the trajectories of the system (29) converge to a compact set S_Σ of radius μ_2, i.e., $\|\Sigma\| \leq \mu_2$ and hence, the trajectories of both (29) and (45) are UUB.

Boundedness of Σ implies boundedness of e, $\dot{e}$ and ϵ; hence e_u, p, $\dot{p}$, Φ_f and Φ_p are also bounded. These facts guarantee boundedness of $\|\dot{E}\|$. The outputs of system (41) under the estimation errors ε and ς are bounded and satisfy

$$y \equiv \ddot{e} + \bar{A}\dot{e} + \bar{B}e - \varepsilon \tag{A.13}$$

$$z \equiv \varsigma - \epsilon \tag{A.14}$$

From (29) and (45) it can be seen that (A.13) and (A.14) are equivalent to $y = \Phi_p^\top\widetilde{\Theta}$ and $z = \Phi_f^\top\widetilde{\Theta}$, respectively. Recall from Theorem 3 that the composite update rule (40) has an exponential stable dynamics under the PE conditions (28) and (42). Furthermore, it can be shown that the error e_u and the estimation error ς act as inputs of the exponentially stable dynamics (40). Then, since e_u and ς are bounded so does the parametric error $\widetilde{\Theta}$. Therefore boundedness of both $\widetilde{\Theta}$ and $\widehat{\Theta}$ is concluded. This completes the proof. □

References

[1] Nematollah Ab Aza, Aref Shahmansoorian, and Mohsen Davoudi. From inverse optimal control to inverse reinforcement learning: A historical review. *Annual Reviews in Control*, 50:119–138, 2020.

[2] Mathieu Brunot, Alexandre Janot, Francisco Carrillo, Joono Cheong, and Jean-Philippe Noël. Output error methods for robot identification. *Journal of Dynamic Systems, Measurement, and Control*, 142(3), 2020.

[3] Carlos Canudas de Wit and A Aubin. Robot parameter identification via sequential hybrid estimation algorithm. *European Control Conference*, pages 444–449, 1991.

[4] Juan Alejandro Flores-Campos, Adolfo Perrusquía, Luis Héctor Hernández-Gómez, Noé González, and Alejandra Armenta-Molina. Constant speed control of slider-crank mechanisms: A joint-task space hybrid control approach. *IEEE Access*, 9:65676–65687, 2021.

[5] Hugues Garnier, Michel Mensler, and Alain Richard. Continuous- time model identification from sampled data: implementation issues and performance evaluation. *International journal of Control*, 76(13):1337–1357, 2003.

[6] Ruben Garrido and Roger Miranda. DC servomechanism parameter identification: A closed loop input error approach. *ISA Transactions*, 51:42–49, 2012.

[7] Maxime Gautier, Alexandre Janot, and Pierre-Olivier Vandanjon. A new closed-loop output error method for parameter identification of robot dynamics. *IEEE Transactions on Control Systems Technology*, 21(2), 2013.

[8] Rolf Isermann and Marco Münchhof. *Identification of dynamic systems: an introduction with applications*, volume 85. Springer, 2011.

[9] Alexandre Janot, Maxime Gautier, Anthony Jubien, and Pierre Olivier Vandanjon. Comparison between the cloe method and the didim method for robots identification. *IEEE Transactions on Control Systems Technology*, 22(5):1935–1941, 2014.

[10] Alexandre Janot, Pierre-Olivier Vandanjon, and Maxime Gautier. Identification of physical parameters and instrumental variables validation with two-stage least squares estimator. *IEEE Transactions on Control Systems Technology*, 21(4):1386–1393, 2012.

[11] Jingfu Jin and Nicholas Gans. Parameter identification for industrial robots with a fast and robust trajectory design approach. *Robotics and Computer-Integrated Manufacturing*, 31:21–29, 2015.

[12] Dawoon Jung, Joono Cheong, Dong Park, and Chanhun Park. Backward sequential approach for dynamic parameter identification of robot manipulators. *International Journal of Advanced Robotic Systems*, 15(1):1–10, 2018.

[13] Rafael Kelly and Victor Santibánez. *Control of Robot Manipulators in Joint space*. Pearson, Prentice Hall, 2003.

[14] Hassan Khalil. *Nonlinear Systems*. Prentice Hall, third edition, 2002.

[15] Ioan Dorè Landau and Alireza Karimi. An output error recursive algorithm for unbiased identification in closed loop. *Automatica*, 33(5):933–938, 1997.

[16] Frank Lewis, Suresh Jagannathan, and Aydin Yeşildirek. *Neural Network control of robot manipulators and nonlinear systems*. Taylor & Francis, 1999.

[17] Lennart Ljung. System identification. In *Signal analysis and prediction*, pages 163–173. Springer, 1998.

[18] Roger Miranda-Colorado and Javier Moreno-Valenzuela. Experimental parameter identification of flexible joint robot manipulators. *Robotica*, 36(3):313–332, 2018.

[19] Benigno Munoz-Barron, Jesus R Rivera-Guillen, Roque A Osornio-Rios, and Rene J Romero-Troncoso. Sensor fusion for joint kinematic estimation in serial robots using encoder, accelerometer and gyroscope. *Journal of Intelligent & Robotic Systems*, 78(3):529–540, 2015.

[20] Oliver Nelles. Nonlinear dynamic system identification. In *Nonlinear System Identification*, pages 831–891. Springer, 2020.

[21] Charles Neuman and Vassilios Tourassis. Discrete dynamic robot models. *IEEE transactions on systems, man, and cybernetics*, SMC-15(2):193–204, 1985.

[22] Adolfo Perrusquía, Juan Alejandro Flores-Campos, and Christopher René Torres San-Miguel. A novel tuning method of PD gravity compensation controller for robot manipulators. *IEEE Access*, 8:114773–114783, 2020.

[23] Adolfo Perrusquía and Wen Yu. Discrete-time $\mathcal{H}_2$ neural control using reinforcement learning. *IEEE Transactions on Neural Networks and Learning Systems*, 2020.

[24] Adolfo Perrusquía and Wen Yu. Human-in-the-loop control using euler angles. *Journal of Intelligent & Robotic Systems*, 97:271–285, 2020.

[25] Adolfo Perrusquía and Wen Yu. Neural $\mathcal{H}_2$ control using continuous-time reinforcement learning. *IEEE Transactions on Cybernetics*, 2020.

[26] Adolfo Perrusquía and Wen Yu. Continuous-time reinforcement learning for robust control under worst-case uncertainty. *International Journal of Systems Science*, 52(4):770–784, 2021.

[27] Adolfo Perrusquía and Wen Yu. Identification and optimal control of nonlinear systems using recurrent neural networks and reinforcement learning: An overview. *Neurocomputing*, 438:145–154, 2021.

[28] Adolfo Perrusquía, Wen Yu, and Alberto Soria. Position/ force control of robot manipulators using reinforcement learning. *Industrial Robot: the international journal of robotics research and application*, 46(2):267–280, 2019.

[29] Adolfo Perrusquía, Wen Yu, Alberto Soria, and Rogelio Lozano. Stable admittance control without inverse kinematics. *20th IFAC World Congress (IFAC2017)*, 50(1):15835–15840, 2017.

[30] Radu-Emil Precup and Stefan Preitl. PI and PID controllers tuning for integral-type servo systems to ensure robust stability and controller robustness. *Electrical Engineering*, 88:149–156, 2006.

[31] Fernando Reyes and Rafael Kelly. Experimental evaluation of identification schemes on a direct drive robot. *Robotica*, 15(5):563–571, 1997.

[32] Shankar Sastry and Marc Bodson. *Adaptive Control, Stability, Convergence and Robustness*. Prentice Hall, 1989.

[33] Shankar Sastry and Marc Bodson. *Adaptive control Stability, Convergence and Robustness*. Prentice Hall Information and System Sciences Series, 1989.

[34] Jean-Jacques Slotine and Weiping Li. On the adaptive control of robot manipulators. *The international journal of robotics research*, 6(3):49–59, 1987.

[35] Jean-Jacques Slotine and Weiping Li. Composite adaptive control of robots manipulators. *Automatica*, 25(4):509–519, 1989.

[36] Jean-Jacques E Slotine and Weiping Li. *Applied Nonlinear Control*. Prentice Hall, 1991.

[37] Mark Spong and Mathukumalli Vidyasagar. *Robot dynamics and control*. John Wiley & Sons, 2008.

[38] Jan Swevers, Chris Ganseman, Joris De Schutter, and Hendrik Van Brussel. Experimental robot identification using optimised periodic trajectories. *Mechanical Systems and Signal Processing*, 10(5):561–577, 1996.

[39] Jan Swevers, Walter Verdonck, and Joris De Schutter. Dynamic model identification for industrial robots. *IEEE control systems magazine*, 27(5):58–71, 2007.

[40] Yu Tang and Marco Arteaga. Adaptive control of robot manipulators based on passivity. *IEEE Transactions on Automatic Control*, 39(9):1871–1875, 1994.

[41] Claudio Urrea and José Pascal. Design and validation of a dynamic parameter identification model for industrial manipulator robots. *Archive of Applied Mechanics*, pages 1–27, 2021.

[42] Hanlei Wang. Adaptive control of robot manipulators with uncertain kinematics and dynamics. *IEEE Transactions on Automatic Control*, 62(2):948–954, 2016.

[43] Wen Yu and Adolfo Perrusquía. Simplified stable admittance control using end-effector orientations. *International Journal of Social Robotics*, 12:1061–1073, 2020.

2022-04-12

Stable robot manipulator parameter identification: a closed-loop input error approach

Perrusquía, Adolfo

Elsevier

Perrusquia A, Garrido R, Yu W. (2022) Stable robot manipulator parameter identification: a closed-loop input error approach. Automatica, Volume 141, July 2022, Article number 110294 https://doi.org/10.1016/j.automatica.2022.110294